Lewis Grant
IN-39
P-23

NASA Contractor Report 185286

Creep and Creep Rupture of Strongly Reinforced Metallic Composites

D.N. Robinson, W.K. Binienda, and M. Miti-Kavuma
University of Akron
Akron, Ohio

August 1990

Prepared for
Lewis Research Center
Under Grant NAG3-379

NASA
National Aeronautics and
Space Administration

(NASA-CR-185286) CREEP AND CREEP RUPTURE OF STRONGLY REINFORCED METALLIC COMPOSITES Final Report (Akron Univ.) 23 p CSCL 20K

N90-28110

Unclas
G3/39 0302647

CREEP AND CREEP RUPTURE OF STRONGLY REINFORCED METALLIC COMPOSITES

By D.N.Robinson[1], W.K.Binienda[2] and M.Miti–Kavuma[3]

ABSTRACT: A creep and creep damage theory is presented for metallic composites with strong fibers. Application is to reinforced structures in which the fiber orientation may vary throughout but a distinct fiber direction can be identified locally (local transverse isotropy). The creep deformation model follows earlier work and is based on a flow potential function that depends on invariants reflecting stress and the material symmetry. As the focus is on the interaction of creep and damage, primary creep is ignored. The creep rupture model is an extension of continuum damage mechanics and includes an isochronous damage function that depends on invariants specifying the local maximum transverse tension and the maximum longitudinal shear stress. It is posited that at high temperature and low stress, appropriate to engineering practice, these stress components damage the fiber/matrix interface through diffusion controlled void growth, eventually causing creep rupture. Experiments are outlined for characterizing a composite through creep rupture tests under transverse tension and longitudinal shear. Application is made to a thin–walled pressure vessel with reinforcing fibers at an arbitrary helical angle. The results illustrate the usefulness of the model as a means of achieving optimal designs of composite structures where creep and creep rupture are life limiting.

INTRODUCTION

When metallic structures operate at temperatures in excess of 0.3 T_m, where T_m is the melting temperature of the metal, it is generally observed that the structure suffers time–dependent deformation and eventually ruptures. For components made of highly creep resistant materials or where distortion is not a controlling factor structural lifetime is often limited by creep rupture.

In design practice, estimates of creep deformation are often based on generalizations of the classical Norton creep law. Predictions of creep failure resulting from material deterioration are frequently based on generalizations of the Kachanov (1958,1986)/ Rabotnov (1969) damage law.

1. Prof., Univ. of Akron, Akron, OH. 44325–3905
2. Asst.Prof., Univ. of Akron, Akron, OH. 44325–3905
3. Grad. Student, Univ. of Akron, Akron, OH. 44325–3905

Generalizations of these laws (e.g., Leckie and Hayhurst (1974), Lemaitre and Chaboche (1985), Leckie (1986)) have been proposed that account for multiaxial stress and that employ damage evolutionary laws reflecting various micromechanisms (Ashby and Dyson(1984)). These generalizations commonly employ concepts such as an effective stress and an isochronous failure function or surface. Important conclusions based on these formulations are that creep deformation, rupture time and failure strain all are influenced strongly by the *multiaxial state of stress.* Further, they conclude that damage evolves more or less *anisotropically* depending on the mechanisms involved.

The objective of this paper is to extend these results concerning creep and creep damage to metals that are reinforced by strong unidirectional fibers. The focus is on reinforced structures where the fiber direction may vary from point to point but that a single material (*fiber*) direction is identifiable locally (viz., *local transverse isotropy*). The strong fibers are assumed to suppress creep along their direction, but in the presence of general states of stress both creep and creep damage occurs.

The representation of creep *deformation* follows earlier work concerning strongly fiber reinforced metals (Robinson and Duffy (1990), and Binienda and Robinson (1990)). Tensorial invariants identified in these works reflecting deviatoric stress dependence and the appropriate material symmetry are adopted in the present flow law. As the emphasis here is on the interaction of creep and damage (*tertiary* creep) the relatively small contribution of *primary* creep (cf.,Petrasek and Titran (1988),Grobstein (1989a,1989b)) is ignored.

A major assumption here is that the stress dependence of *damage evolution* is, (i) on the *maximum tensile stress normal to the local fiber direction* and, (ii) on the *maximum longitudinal shear stress,* i.e., the maximum shear stress on planes containing the fibers and in a direction along the fibers. It is postulated that the effects of these stress components interact to damage the composite internally (along the fiber / matrix interface), eventually leading to creep rupture. Under this idealization, tensile stress along the fibers causes no creep and no damage; tensile stress (*however small*) transverse to the fibers causes both creep deformation and damage. In reality, stress along the fibers causes damage and leads to a finite lifetime, however, the difference in damage rates, and thus rupture times, under longitudinal and transverse stress generally exceeds an order of magnitude (Grobstein (1989a), Petrasek and Titran (1988)).

Studies of creep damage of some monolithic alloys suggest that at lower stress levels appropriate to engineering practice, creep rupture occurs mainly by intergranular void growth (Cocks and Ashby (1982)). In such cases void growth rates at a particular grain boundary are controlled by diffusion mechanisms which, in turn, are controlled by the *maximum tensile stress transverse to the given grain boundary* (Hull and Rimmer (1959), Chuang and Rice(1973)). Here, we postulate that the fiber–matrix interface in a metallic composite plays a role, on the *mesostructural* scale, analogous to that of grain boundaries on the *microstructural* scale. Thus, at high temperature and lower stress levels, we anticipate that the *maximum tensile stress transverse to the fiber direction* may strongly influence void growth at the fiber–matrix interface and, consequently may correlate with a creep rupture mechanism based on interfacial degradation through diffusion related void growth. It is expected that the diffusion mechanisms involved may include those known to control void growth rates at grain boundaries as well as other *meso*mechanisms observed to be present in metallic composite systems, e.g., those leading to phenomena such as Kirkendall porosity or the evolution of an interphase (Grobstein (1989b)). As indicated earlier, account is also taken of the contribution of *longitudinal shear stress* to interfacial degradation. These stress dependencies of damage evolution are included by introducing invariants that correspond to the local maximum transverse tension and longitudinal shear. These invariants are taken as arguments of an *isochronous damage function* (cf.Leckie (1986)).

As the damage invariants depend on the local stress and material orientation, the *rate of damage evolution is anisotropic.* Thus, *rupture time* and *failure strain* depend similarly on *fiber orientation.* The *degree* of damage is measured by a *scalar* (Kachanov (1958)) and thus does not reflect material directionality. Potentially, this may lead to inaccuracies in life prediction of structures subjected to highly *non–proportional* loading; it is expected that this will *not* seriously affect life prediction of proportionally loaded structures, e.g., pressure vessels, (cf.,Ho (1987)).

Following the development of the creep /creep rupture model, experiments are outlined for the determination of the material parameters and functions. Application is then made to a simple structure i.e., a thin – walled tubular pressure vessel.

THE CREEP/CREEP DAMAGE MODEL

The form of the creep deformation / damage model proposed by Leckie and Hayhurst (1974) is extended for metallic composites. We consider high–temperature, isothermal conditions and a composite of given fiber volume percentage. Generalization to nonisothermal conditions follows as in Cocks and Ponter (1987). Extension to other fiber densities is possible by considering key material parameters as functions of fiber volume percentage.

Invariants identified in Robinson and Duffy (1990) and Binienda and Robinson (1990) are adopted to account for material directionality (*local transverse isotropy*). As earlier, an orientation tensor

$$D_{ij} = d_i d_j \tag{1}$$

is introduced where d_i (i=1,2,3) are the components of a unit vector denoting the local fiber direction. The invariants I_1 and I_2 are defined as (cf., Robinson and Duffy (1990))

$$\left.\begin{aligned} I_1 &= J_2 + \frac{1}{4} I^2 - \mathcal{J} \\ I_2 &= \mathcal{J} - I^2 \end{aligned}\right\} \tag{2}$$

in which

$$J_2 = \frac{1}{2} s_{ij}s_{ji} \qquad I = D_{ij}s_{ji} \qquad \mathcal{J} = D_{ij}s_{jk}s_{ki} \tag{3}$$

and s_{ij} = the components of the deviatoric stress. The physical meanings of I_1 and I_2 are:

$$\sqrt{I_1} \equiv S = \text{the } \textit{maximum transverse shear stress} \tag{4}$$

$$\sqrt{I_2} \equiv \mathcal{S} = \text{the } \textit{maximum longitudinal shear stress} \tag{5}$$

We define an additional invariant as

$$\mathcal{N} = \left\langle \frac{1}{2}(\mathcal{I}_1 - \mathcal{I}_2) + S \right\rangle \tag{6}$$

where

$$\mathcal{I}_1 = \sigma_{ii} \qquad \mathcal{I}_2 = D_{ij}\sigma_{ji} \tag{7}$$

and

$$\langle x \rangle = \begin{cases} x\,; & x > 0 \\ 0\,; & x \leq 0 \end{cases}$$

Physically,

$$\mathcal{N} = \text{the } \textit{maximum transverse tensile stress} \tag{8}$$

These invariants enter the model through two functions $\phi(\sigma_{ij},D_{ij})$ — the *flow potential* function and $\Delta(\sigma_{ij},D_{ij})$ — the *isochronous failure* function. Guided by Binienda and Robinson (1990) we take ϕ as:

$$\phi = \frac{2}{\sigma_0}\sqrt{J_2 - \frac{3}{4}I^2} \tag{9}$$

where σ_0 is a reference stress to be defined subsequently. Consistent with the discussion in the previous section, the function Δ is taken to depend on the invariants $\mathcal{N}$ and $\mathcal{S}$. The surface $\Delta(\mathcal{N},\mathcal{S}) = 1$ in the $\mathcal{N},\mathcal{S}$ space will be termed the *isochronous failure surface.* A specific functional form of Δ for a given material must be determined by experiment. Possible experiments for this purpose might employ reinforced thin–walled tubes of the composite of interest subjected to combined tension, torsion and pressure. As pertinent experimental results are not available currently, here, in the interest of simplicity, we adopt a *linear* form (fig.1)

$$\Delta = \frac{1}{\sigma_0}(\mathcal{N} + \alpha\,\mathcal{S}) \tag{10}$$

in which α is a material constant.

A modified Calladine and Drucker (1962) *potential* form serves as the *flow law* i.e.,

$$\frac{\dot{\epsilon}_{ij}}{\dot{\epsilon}_0} = \phi^n \frac{\partial\phi}{\partial(\sigma_{ij}/\sigma_0)}\frac{1}{\Psi^n} \tag{11}$$

With ϕ ,eq. (9), into eq.(11) there results

$$\frac{\dot{\epsilon}_{ij}}{\dot{\epsilon}_0} = 2\,\phi^{n-1}\frac{\Gamma_{ij}}{\sigma_0}\frac{1}{\Psi^n} \tag{12}$$

where

$$\Gamma_{ij} = s_{ij} - \frac{I}{2}(3D_{ij} - \delta_{ij}) \tag{13}$$

The *evolutionary law* is taken as (cf., Leckie (1986)):

$$\dot{\Psi} = -\left(\frac{\lambda - 1}{n\lambda t_0}\right)\Delta^{\nu}\frac{1}{\Psi^m} \tag{14}$$

in which

$$m = \frac{n\lambda}{\lambda - 1} - 1 \tag{15}$$

The scalar Ψ is the material *continuity* (Kachanov (1958)); it equals unity for a material element entirely intact and zero for an element having lost load carrying capacity entirely.

As indicated earlier, σ_0 is a reference stress and

$$\dot{\epsilon}_0, t_0, \lambda, n, \nu \text{ and } \alpha$$

are material constants; their physical meanings and their determination are the subjects of the following section.

An alternative and useful form of the flow law, eq.(12) can be stated by defining an *effective stress*

$$\bar{\sigma} = \sqrt{2\,\Gamma_{ij}\Gamma_{ji}} \tag{16}$$

and an *effective inelastic strain*

$$\bar{\epsilon} = \sqrt{\frac{1}{2}\,\epsilon_{ij}\epsilon_{ji}} \tag{17}$$

Using eq.(13), the flow law can then be written

$$\frac{\dot{\bar{\epsilon}}}{\dot{\epsilon}_0} = \left(\frac{\bar{\sigma}}{\sigma_0\Psi}\right)^n = \left(\frac{\phi}{\Psi}\right)^n \tag{18}$$

relating the effective stress and effective inelastic strain rate.

For the limiting case of *isotropy*, the creep / creep rupture model expressed in eqs. (9)–(15) reduces to that proposed by Leckie and Hayhurst (1974) and Leckie (1986) for isotropic alloys. This reduction is discussed in the Appendix.

DETERMINATION OF THE MATERIAL CONSTANTS

The model expressed in eqs. (9)–(15) predicts *no creep* and *no damage* under a constant longitudinal tension (fig. 2a). Under a *transverse tensile stress* $\sigma_{22} = \sigma$ (fig. 2b) , the model reduces to

$$\frac{\dot{\epsilon}}{\dot{\epsilon}_0} = \left(\frac{\sigma}{\sigma_0\Psi}\right)^n \tag{19}$$

$$\dot{\Psi} = -\left(\frac{\lambda - 1}{n\lambda t_0}\right)\left(\frac{\sigma}{\sigma_0}\right)^{\nu}\frac{1}{\Psi^m}\,; \qquad m = \frac{\lambda n}{\lambda - 1} - 1 \tag{20}$$

where $\dot{\epsilon} = \dot{\epsilon}_{22}$ = the transverse creep rate (fig. 2b). With $\sigma = \sigma_0$ i,e,. at the *reference* transverse stress, and with $\Psi = 1$,i.e., for an *undamaged* material, eq. (19) gives $\dot{\epsilon} = \dot{\epsilon}_0$. Thus, the constant $\dot{\epsilon}_0$ represents the (*early*) creep rate under the transverse reference stress σ_0 (fig. 3).

Again, with $\sigma = \sigma_0$ eq. (20) can be integrated from $\Psi = 1$ to Ψ giving

$$\Psi^n = (1 - \frac{t}{t_0})^{\frac{\lambda-1}{\lambda}} \tag{21}$$

At failure ($t = t_f$ and $\Psi = 0$) we have $t_f = t_0$ from eq. (21). Thus, t_0 denotes the time to failure under the reference (*transverse*) stress σ_0 (fig. 2b).

Inserting eq. (21) into eq. (19) with $\sigma = \sigma_0$ results in

$$\frac{\dot{\epsilon}}{\dot{\epsilon}_0} = (1 - \frac{t}{t_0})^{\frac{1-\lambda}{\lambda}} \tag{22}$$

Integrating eq. (22) over $t = 0 \rightarrow t_0$ and $\epsilon = 0 \rightarrow \epsilon_f$, we get for the *transverse failure strain* ϵ_f

$$\frac{\epsilon_f}{\dot{\epsilon}_0} = \lambda t_0 \tag{23}$$

or

$$\lambda = \frac{\epsilon_f}{\dot{\epsilon}_0 t_0} \tag{24}$$

The constant λ is referred to as the *creep damage tolerance* in the literature on creep of monolithic alloys (cf., Leckie (1986)). In effect, λ measures the ability of the metal to withstand local straining at points of high strain concentration in a structure. In design practice it is desirable that $\lambda > 10$.

Now we consider an arbitrary transverse tensile stress σ not equal to the reference stress σ_0. For $\Psi = 1$, eq. (19) then reduces to a simple Norton power law. With the constants σ_0 and $\dot{\epsilon}_0$ known and data pairs $(\sigma, \dot{\epsilon})$ measured from the *early* stages of a set of transverse creep rupture tests, an *optimal* value of the exponent n can be determined.

Next, we focus on eq. (20) with σ not equal to σ_0. Integrating over the lifetime $\Psi = 1 \rightarrow 0$ and $t = 0 \rightarrow t_f$ we obtain

$$\frac{t_f}{t_0} = \frac{1}{(\sigma/\sigma_0)^{\nu}} \tag{25}$$

Again, with σ_0 and t_0 known and the data pairs (σ, t_f) measured from a set of transverse creep rupture tests, an optimal value of ν can be obtained. At this point, the only remaining constant to be specified is α in eq. (10).

Under a constant *longitudinal shear stress* $\sigma_{12} = \tau$ (fig. 2c), eq. (14) reduces to

$$\dot{\Psi} = -\left(\frac{\lambda - 1}{n\lambda t_0}\right)\left(\frac{\alpha\tau}{\sigma_0}\right)^{\nu}\frac{1}{\Psi^m} ; \qquad m = \frac{\lambda n}{\lambda - 1} - 1 \tag{26}$$

Integrating eq. (26) over $\Psi = 1 \to 0$ and $t = 0 \to t_f$ there results

$$\frac{t_f}{t_0} = \frac{1}{(\alpha\tau/\sigma_0)^{\nu}} \tag{27}$$

Combining eq. (25) and eq. (27) and solving for α we get

$$\alpha = \frac{\sigma}{\tau}\left(\frac{t_f^{tt}}{t_f^{ls}}\right)^{\frac{1}{\nu}} \tag{28}$$

where, for purposes of identification, t_f^{tt} corresponds to the time to failure under the *transverse tension* σ (from eq. (25)) and t_f^{ls} corresponds to the time to failure under the *longitudinal shear* τ (from eq. (27)). If we have several data pairs (σ, t_f^{tt}) and (τ, t_f^{ls}) and ν is known, we can find an optimal value of α . In particular, if σ and τ lie on the *isochronous failure surface* $\Delta = 1$ then $t_f^{tt} = t_f^{ls} = t_0$ and, from eq. (28), $\alpha = \sigma/\tau$. This completes the procedure for specifying the material constants.

CREEP RUPTURE UNDER MULTIAXIAL STRESS

We now examine creep rupture under a constant *multiaxial* stress. For fixed fiber orientation the functions $\phi(\sigma_{ij}/\sigma_o, D_{ij})$ and $\Delta(\sigma_{ij}/\sigma_o, D_{ij})$ are then constant. Eq. (14) can thus be integrated over $t = 0 \to t$ and $\Psi = 1 \to \Psi$ providing (cf,eq. (21))

$$\Psi^n = \left(1 - \Delta^{\nu}\frac{t}{t_0}\right)^{\frac{\lambda-1}{\lambda}} \tag{29}$$

At failure ($t = t_f$ and $\Psi = 0$) eq. (29) gives

$$\frac{t_f}{t_o} = \frac{1}{\Delta^{\nu}} \tag{30}$$

We recall that for $\Delta = 1$, viz., a stress state on the isochronous failure surface, $t_f = t_o$.

Now consider the alternative form of the flow law expressed in eq. (18). With ϕ = constant and making use of eq. (29), eq.(18) can be integrated over $t = 0 \to t_f$ and $\bar{\epsilon} = 0 \to \bar{\epsilon}_f$ as follows

$$\int_0^{\bar{\epsilon}_f} \frac{d\bar{\epsilon}}{\dot{\epsilon}_o} = \phi^n \int_0^{t_f} (1 - \Delta^{\nu}\frac{t}{t_o})^{\frac{1-\lambda}{\lambda}} dt \tag{31}$$

Using eq. (30) in eq. (31) results in

$$\frac{\bar{\epsilon}_f}{\dot{\epsilon}_o} = \phi^n \lambda t_f \tag{32}$$

Then using eq. (24), we have

$$\frac{\bar{\epsilon}_f}{\epsilon_f} = \frac{\phi^n}{\Delta^{\nu}} \tag{33}$$

Eqs. (30) and (33) show that the time to failure $t_f(\sigma_{ij}/\sigma_o, D_{ij})$ and the effective failure strain $\bar{\epsilon}_f(\sigma_{ij}/\sigma_o, D_{ij})$ are functions of the *multiaxial stress* and the *fiber orientation*. In principle, for a given stress state the fiber direction can be chosen to *optimize* t_f and $\bar{\epsilon}_f$ in accordance with eqs. (30) and (33) and an appropriate design criterion.

In the next section we apply the theory presented here to a fiber reinforced thin–walled tubular pressure vessel. There we calculate t_f using eq. (30) and $\bar{\epsilon}_f$ using eq. (33) for the tubular vessel having a single family of strong helical fibers oriented arbitrarily.

APPLICATION TO A THIN–WALLED PRESSURE VESSEL

Consider a thin–walled tube with closed ends that is subjected to an interior pressure p. The tube with radius R and wall thickness h is reinforced with a family of strong helical fibers making an angle θ with the circumferential direction x_2 (fig. 4). Taking

$$\frac{pR}{h} = \sigma, \tag{34}$$

the stress components σ_{ij} and the deviatoric stress components s_{ij} in the tube wall are, respectively

$$\left.\begin{array}{ll} \sigma_{11} = \frac{\sigma}{2} \qquad \sigma_{22} = \sigma & s_{22} = -s_{33} = \frac{\sigma}{2} \\ \sigma_{33} = \sigma_{12} = \sigma_{13} = \sigma_{23} = 0 & s_{11} = s_{12} = s_{13} = s_{23} = 0 \end{array}\right\} \tag{35}$$

The components of the orientation tensor D_{ij} are (fig. 4)

$$\left.\begin{array}{c} D_{11} = \sin^2\theta, \quad D_{22} = \cos^2\theta, \quad D_{12} = \sin\theta\cos\theta \\ D_{33} = D_{13} = D_{23} = 0 \end{array}\right\} \tag{36}$$

The relevant invariants can then be calculated,

$$\left.\begin{array}{l} J_2 = \frac{\sigma^2}{4} \\ I^2 = \frac{\sigma^2}{4}\cos^4\theta \end{array}\right\} \tag{37}$$

giving, from eq. (9)

$$\phi = \frac{\sigma}{\sigma_0}\sqrt{1 - \frac{3}{4}\cos^4\theta} \tag{38}$$

Additional invariants are

$$\left.\begin{array}{l} S = \frac{\sigma}{4}(\,2 - \cos^2\theta\,) \\ \mathscr{S}_b = \sigma\,(\,\cos^2\theta + \frac{1}{2}\sin^2\theta\,) \\ \mathscr{S}_a = \frac{3}{2}\,\sigma \end{array}\right\} \tag{39}$$

leading to

$$\mathscr{N} = \sigma\,(\,1 - \frac{1}{2}\cos^2\theta\,) \tag{40}$$

Finally,

$$\mathscr{S} = \frac{\sigma}{4}\sin 2\theta \tag{41}$$

and from eq. (10)

$$\Delta = \frac{\sigma}{\sigma_0}\left(1 - \frac{1}{2}\cos^2\theta + \frac{\alpha}{4}\sin 2\theta \right) \tag{42}$$

Using eqs. (30), (34) and (42) we write the *dimensionless rupture time* vs. fiber angle θ as

$$\left(\frac{t_f}{t_o}\right)^{\frac{1}{\nu}} \frac{pR}{\sigma_o h} = \frac{1}{1 - \frac{1}{2}\cos^2\theta + \frac{\alpha}{4}\sin 2\theta} \tag{43}$$

Evaluating eq. (43) for $\theta = 0^o$ (circumferential reinforcement) and $\theta = 90^o$ (longitudinal reinforcement) and forming the ratio of these results, we get for any pressure p,

$$\frac{t_f(0^o)}{t_f(90^o)} = 2^{\nu} \tag{44}$$

Thus, the failure time for circumferential fiber strengthening may exceed substantially that for longitudinal strengthening. Typically, $\nu \approx 9$ so that $2^{\nu} \approx 512$.

A graph of eq. (43) is shown in fig. 5. The three curves shown are for $\alpha = 0$, 1/2 and 1. The first, $\alpha = 0$, implies that *no damage* results from the *maximum longitudinal shear* $\mathscr{S}$. The last condition, $\alpha = 1$, implies that $\mathscr{S}$ and the *maximum transverse tension* $\mathscr{N}$ are equally damaging.

Fig. 5 shows that for $\alpha = 0$ the rupture time decreases monotonically with increasing fiber angle θ. When longitudinal shear $\mathscr{S}$ contributes to creep damage, viz., $\alpha = 1/2$ or 1, fig. 5 shows that the rupture time no longer decreases monotonically with θ but exhibits a *minimum* value at an intermediate fiber angle.

Combining eqs. (33), (38) and (42) we obtain the *dimensionless effective failure strain* vs. θ, viz.,

$$\frac{\bar{\epsilon}_f}{\epsilon_f}\left(\frac{pR}{\sigma_o h}\right)^{\nu - n} = \frac{\left(\sqrt{1 - \frac{3}{4}\cos^4\theta}\right)^n}{\left(1 - \frac{1}{2}\cos^2\theta + \frac{\alpha}{4}\sin 2\theta\right)^{\nu}} \tag{45}$$

Similarly evaluating eq. (45) for $\theta = 0^o$ and $\theta = 90^o$ and taking the ratio of these results, we have for any pressure p.

$$\frac{\bar{\epsilon}_f(0^o)}{\bar{\epsilon}_f(90^o)} = 2^{\nu-n} \tag{46}$$

Now for definiteness we consider specific values of the exponents $n = 6$ and $\nu = 9$ and take the pressure as $pR/\sigma_0 h = 1$. The result is plotted in fig.8. As earlier, three curves are shown corresponding to $\alpha = 0$, 1/2 and 1. With the given values of p,n and ν each curve shows $\bar{\epsilon}_f = \epsilon_f$ at $\theta = 90^O$ i.e., the *effective failure strain* is equal to that corresponding to transverse tension at the *reference stress* σ_0. At $\theta = 0^O$ each curve shows $\bar{\epsilon}_f = 2^{9-6}\epsilon_f = 8\ \epsilon_f$, consistent with eq. (46).

For the curve $a = 0$ in fig. 6, $\bar{\epsilon}_f$ reaches a *maximum* of $\approx 14\ \epsilon_f$ at $\theta \approx 25^O$; conversely, the curves $a = 1/2$ and 1 each exhibit a *minim*um at an intermediate fiber angle.

The simple structure considered in this section is not of essential practical importance but serves as an illustrative example of the dependence of t_f and $\bar{\epsilon}_f$ (or equivalently, an *effective creep damage tolerance* $\bar{\lambda} = (\bar{\epsilon}_f/\epsilon_f)\ \lambda$) on the multiaxial (*biaxial*) stress state and on the *fiber orientation.* In a general design situation we may want to maximize both t_f and $\bar{\epsilon}_f$ (or $\bar{\lambda}$), i.e., we may want a long structural lifetime *and* a large tolerance to local straining at possible strain concentrations. In our present example, we see by comparing figs. 5 and 6 that these maxima do not always occur at a common fiber angle θ , suggesting the necessity of a design compromise in the selection of the optimal fiber orientation. It is intended that the simple model presented here may provide guidance for the practicing structural engineer in making such design considerations.

SUMMARY AND CONCLUSIONS

A creep and creep damage model is presented for metallic composites with strong fibers. The intended applications are reinforced structures in which the fiber direction may vary throughout but a single fiber direction can be identified locally (*local transverse isotropy*).

The representation of creep *deformation* follows earlier work and includes a *flow potential function* ϕ that depends on invariants reflecting the local stress and material orientation. As the focus is on the interaction of creep and damage, the relatively minor role of primary creep is ignored.

The creep *rupture* model is a generalization of classical continuum damage mechanics and includes an *isochronous damage function* Δ taken to depend on invariants specifying the *maximum tensile stress normal to the local fiber direction and the maximum longitudinal shear stress.* These stress components are assumed to damage the composite at the fiber/matrix interface, eventually causing creep rupture. It is conjectured that at high temperature and low stress the fiber/matrix interface plays a role, on the *mesostructural* scale, analogous to grain boundaries on the *microstructural* scale. An anisotropic damage mechanism is posited where interfacial degradation occurs through diffusion (*and hence stress*) controlled void growth, e.g., Kirkendall void growth.

A procedure is outlined for the determination of the several material parameters on the basis of creep rupture testing under *transverse tension.* Additional testing is required to determine the functional dependence and form of the *isochronous damage function.* Here, a *linear* form is assumed requiring a limited number of creep rupture tests under *longitudinal shear.*

General results are obtained for the *time to failure* t_f and the *final effective failure strain* $\bar{\epsilon}_f$ under constant *multiaxial* stress; each is found to depend not only on stress, but on *fiber orientation.* Thus, for a given stress state, the model permits the selection of a fiber orientation that may *optimize* t_f and/or $\bar{\epsilon}_f$ according to a relevant design criterion.

The theory is applied to a thin–walled tubular pressure vessel with strong fibers at an arbitrary helical angle. The quantities t_f and $\bar{\epsilon}_f$ are calculated for the thin tube as functions of fiber angle. As anticipated, the rupture time t_f is a *maximimum* for *circumferential* reinforcement of the tube. Depending on the relative strength of the contributions of *transverse tension* and *longitudinal shear* to the evolution of damage (viz., the form of the *isochronous damage function* Δ) t_f may reach a *minimum* at an intermediate fiber angle (fig. 5). The effective final strain $\bar{\epsilon}_f$ can achieve a *maximum* or a *minimum* at an intermediate angle, again depending on the relative importance of transverse tensile and longitudinal shear damage (fig. 6). In general, simultaneous optimization of t_f and $\bar{\epsilon}_f$ results in a design compromise.

The example problem illustrates the potential usefulness of the proposed model as a means of realizing optimal designs of composite structures where creep and creep rupture are life limiting. Of course, the accuracy of predictions made using the theory depends intimately on the forms of the functions ϕ and Δ and on the material constants. Correct choices of these functions and parameters for a given composite material rest on careful experimentation. Some experimental justification for the choice of ϕ is provided in Binienda and Robinson (1990). However, the functional dependence and form of the isochronous damage function Δ is largely conjectural, particularly the linear form adopted here, and must be verified on the basis of detailed *phenomenological* and *microstructural* observation. Key verification experiments are currently being defined.

ACKNOWLEDGEMENT

The authors acknowledge the support and encouragement of the NASA–Lewis Research Center in the pursuit of this research, especially J.R. Ellis and S.M. Arnold. Prof. D.N. Robinson acknowledges support through NASA grant NAG–3–379.

APPENDIX A. REFERENCES

Ashby,M.F. and Dyson,B.F. (1984), *Creep damage mechanics and micro–mechanics.*, Proc.4^{th}Int.Conf.on Fracture, New Delhi.

Binienda,W.K. and Robinson,D.N. (1990), *A creep model for metallic composites based on matrix testing: Application to Kanthal composites.*,to appear J.Engr.Mech. ASCE.

Calladine,C.R. and Drucker,D.C. (1962), *Nesting surfaces of constant rate of energy dissipation in creep.*, Q.appl.Math.,20,1.

Chuang,T–J. and Rice,J.R. (1973), *The shape of intergranular creep cracks growing by surface diffusion.*, Acta Met.,21.

Cocks,A.C.F. and Ashby,M.F. (1982), *On creep fracture by void growth.*, Prog.Mat.Sci.,27.

Cocks A. C. F. and Ponter A. R. S. (1987), *Creep Deformation and Failure Under Cyclic Thermal Loading*, Report 87–9 University of Leicester, Dept. of Engr. (to appear J. Engr. and Design).

Grobstein,T.L. (1989a), *Creep behavior of Tungsten fiber reinforced Niobium metal matrix composites.*, NASA TM – 102307.

Grobstein,T.L. (1989b), *The interface in Tungsten fiber reinforced Niobium metal matrix composites.*, NASA TM – 102122.

Ho,K–I., (1987), *An anisotropic contiuum damage model for creep dominated multiaxial loading histories.*,Ph.D. Thesis, Georgia Inst. Tech.,8803701.

Hull,D. and Rimmer,D.E. (1959), *The growth of grain boundary voids under stress.*,Phil.Mag.,8.

Kachanov,L.M. (1958), *Time of the fracture process under creep conditions.*, Izv.Akad.Nauk SSR O.T.N. Tekh.Nauk, 8,26.

Kachanov,L.M. (1986), *Introduction to contiuum damage mechanics.*, Martinus – Nijhoff.

Leckie,F.A. and Hayhurst,D.R. (1974), *Creep rupture in structures.*, Proc.R.Soc.Lond., A340.

Leckie,F.A. (1986), *The micro– and macromechanics of creep rupture.*, Engr.Fracture Mech., 25,5.

Lemaitre,J. and Chaboche,J.L. (1985), *Mechanique des materiaux solides.*, Dunod,Paris.

Petrasek,D.W. and Titran,R.H. (1988), *Creep behavior of Tungsten / Niobium and Tungsten / Niobium – 1 percent Zirconium composites.*, NASA TM – 100804.

Rabotnov,Y.N. (1969), *Creep problems in structural members.*, North – Holland, Amsterdam.

Robinson,D.N. and Duffy,S.F. (1990), *Continuum deformation theory for high temperature metallic composites.*, J.Engr.Mech.ASCE, 16,4.

APPENDIX B. ISOTROPIC LIMIT

The *isotropic* limit of the model expressed in eqs. (9) – (15) is found by taking D_{ij} to be an *isotropic tensor* with $D_{ii} = 1$, i.e., $D_{ij} = \frac{1}{3}\delta_{ij}$. Under this limit ϕ in eq. (9) becomes

$$\phi = \frac{2}{\sigma_0}\sqrt{J_2} \tag{1B}$$

and Γ_{ij} in eq. (13) is

$$\Gamma_{ij} = s_{ij} \tag{2B}$$

Following Binienda and Robinson (1990), we define a *new reference stress* σ_0' and a corresponding creep rate $\dot{\epsilon}_0'$ as

$$\sigma_0' = \frac{\sqrt{3}}{2}\sigma_0 \tag{3B}$$

$$\dot{\epsilon}_0' = \frac{2}{\sqrt{3}}\dot{\epsilon}_0 \tag{4B}$$

With these definitions ϕ, eq. (1B), becomes

$$\phi = \frac{\sqrt{3J_2}}{\sigma_0'} \tag{5B}$$

and the flow law eq. (12) reduces to

$$\frac{\dot{\epsilon}_{ij}}{\dot{\epsilon}_0'} = \frac{3}{2}\phi^{n-1}\frac{s_{ij}}{\sigma_0'}\frac{1}{\Psi^n} \tag{6B}$$

as in Leckie and Hayhurst (1974) and Leckie (1986).

Similarly, eqs. (14) and (15) reduce to those of Leckie (1986) with the function Δ, eq. (10), taken as

$$\Delta = \phi = \frac{\sqrt{3J_2}}{\sigma_0'} \qquad \text{or} \qquad \Delta = \frac{\sigma_{max}}{\sigma_0'} \tag{7B}$$

where σ_{max} = the *maximum (tensile) principal stress.*

We note from eq. (3B) that the ratio of the reference stress σ_0' of the isotropic limit to the (*transverse*) reference stress σ_0 of the anisotropic composite is $\sqrt{3}/2$. This result is expected in that the material deforms as a J_2 (*von Mises*) material in the isotropic limit (cf., eq. (5B)) whereas under the constraint of the strong fibers it is forced to deform in transverse tension as a maximum shear stress (*Tresca*) material. The creep (or yield) strengths of these material idealizations are in the same ratio $\sqrt{3}/2$.

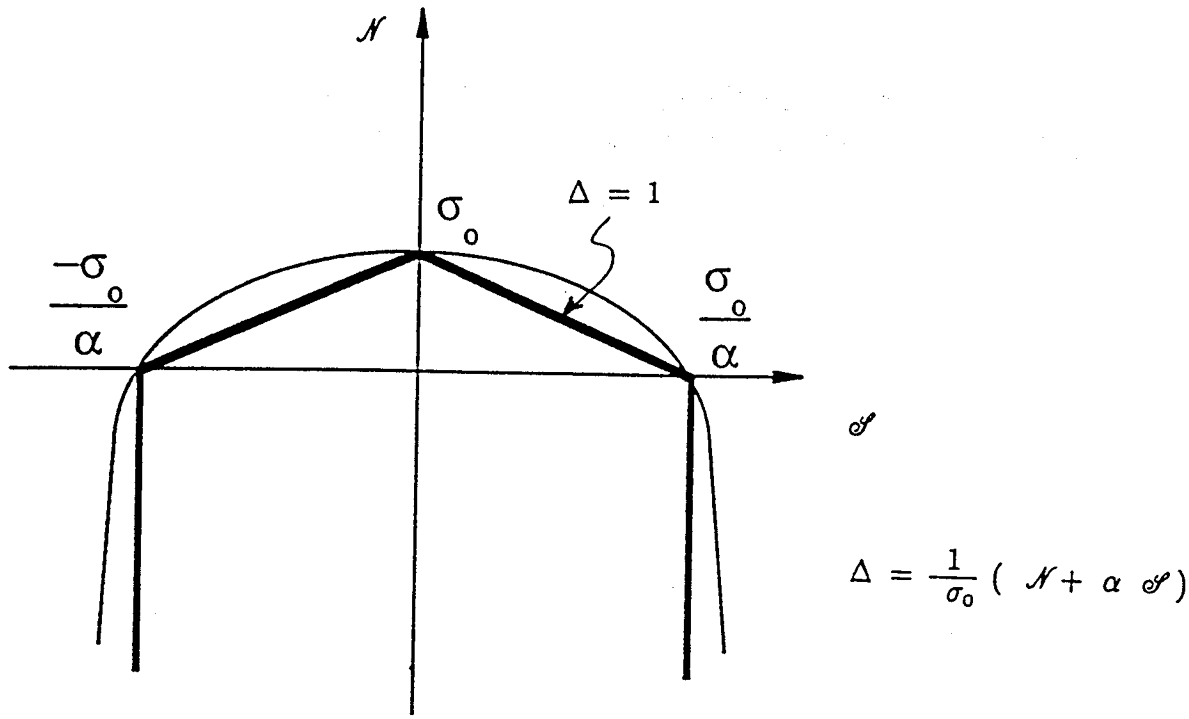

Figure 1. Piecewise Linear isochronous failure surface.

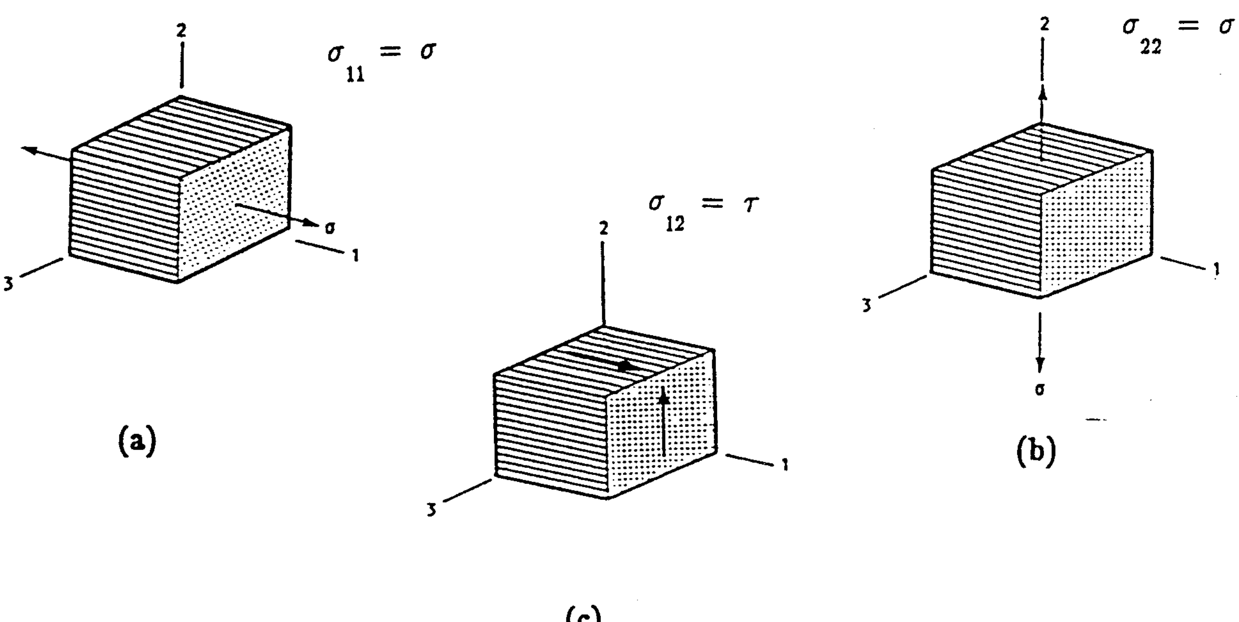

Figure 2. Stress states: (a) longitudinal tension, (b) transverse tension, (c) longitudinal shear.

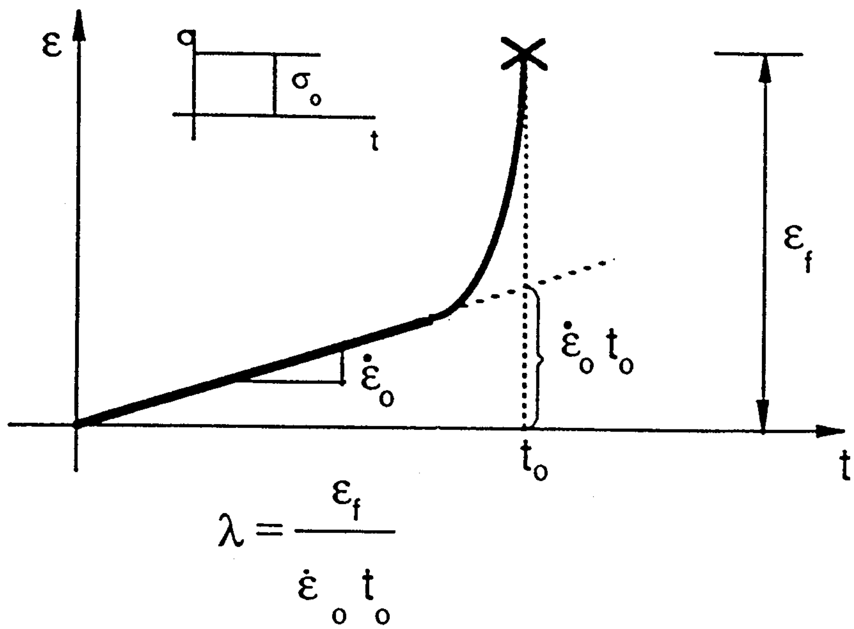

Figure 3. Creep response under reference transverse stress σ_0.

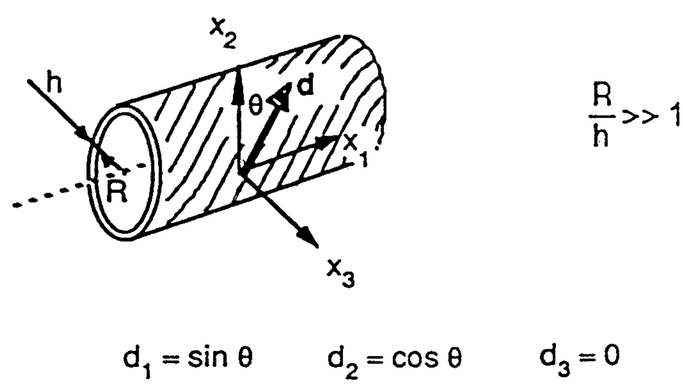

Figure 4 Helically reinforced thin–walled tube under interior pressure p. $\underline{d}$ denotes local fiber direction.

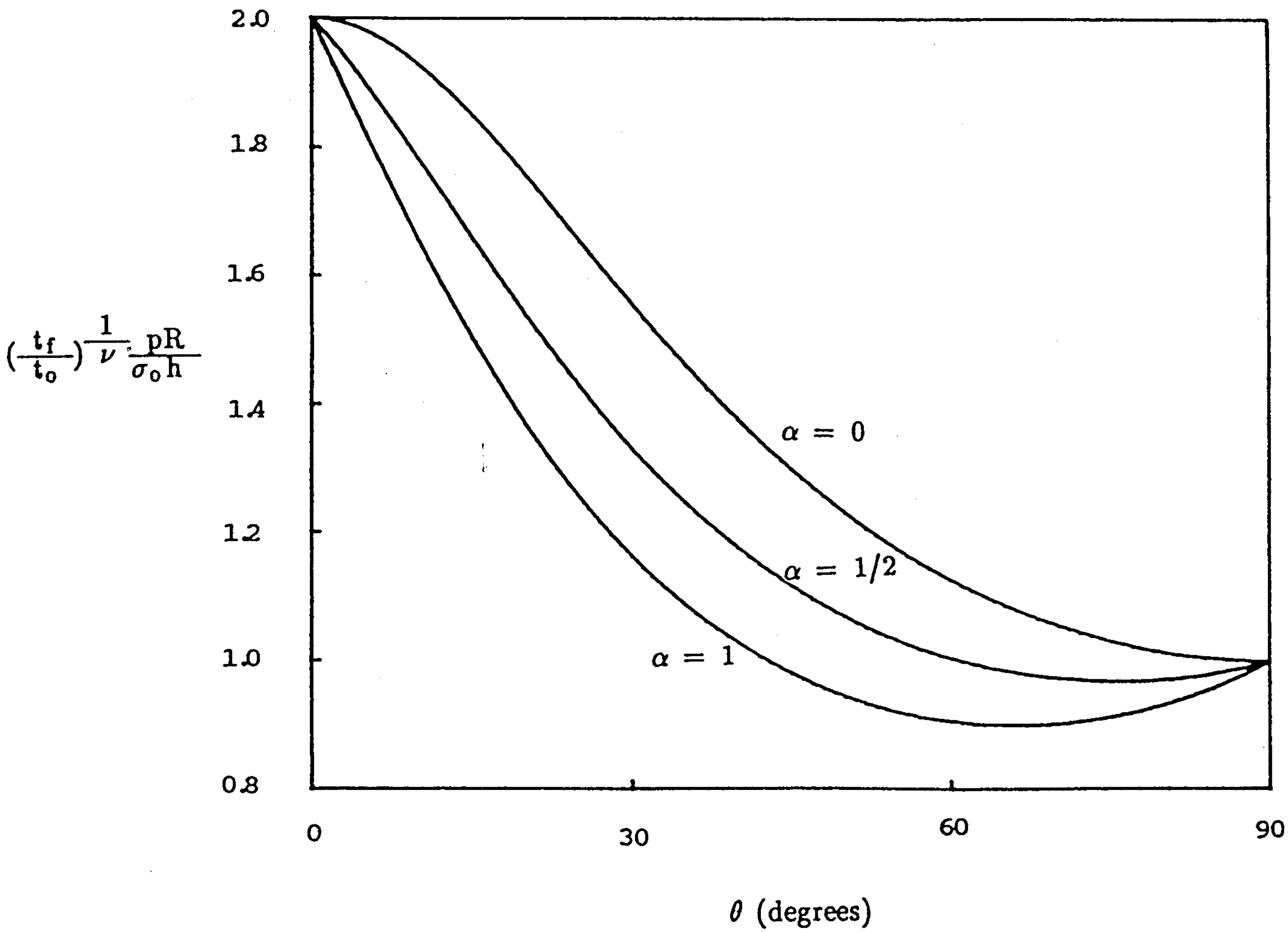

Figure 5. Dimensionless rupture time vs. fiber angle θ.

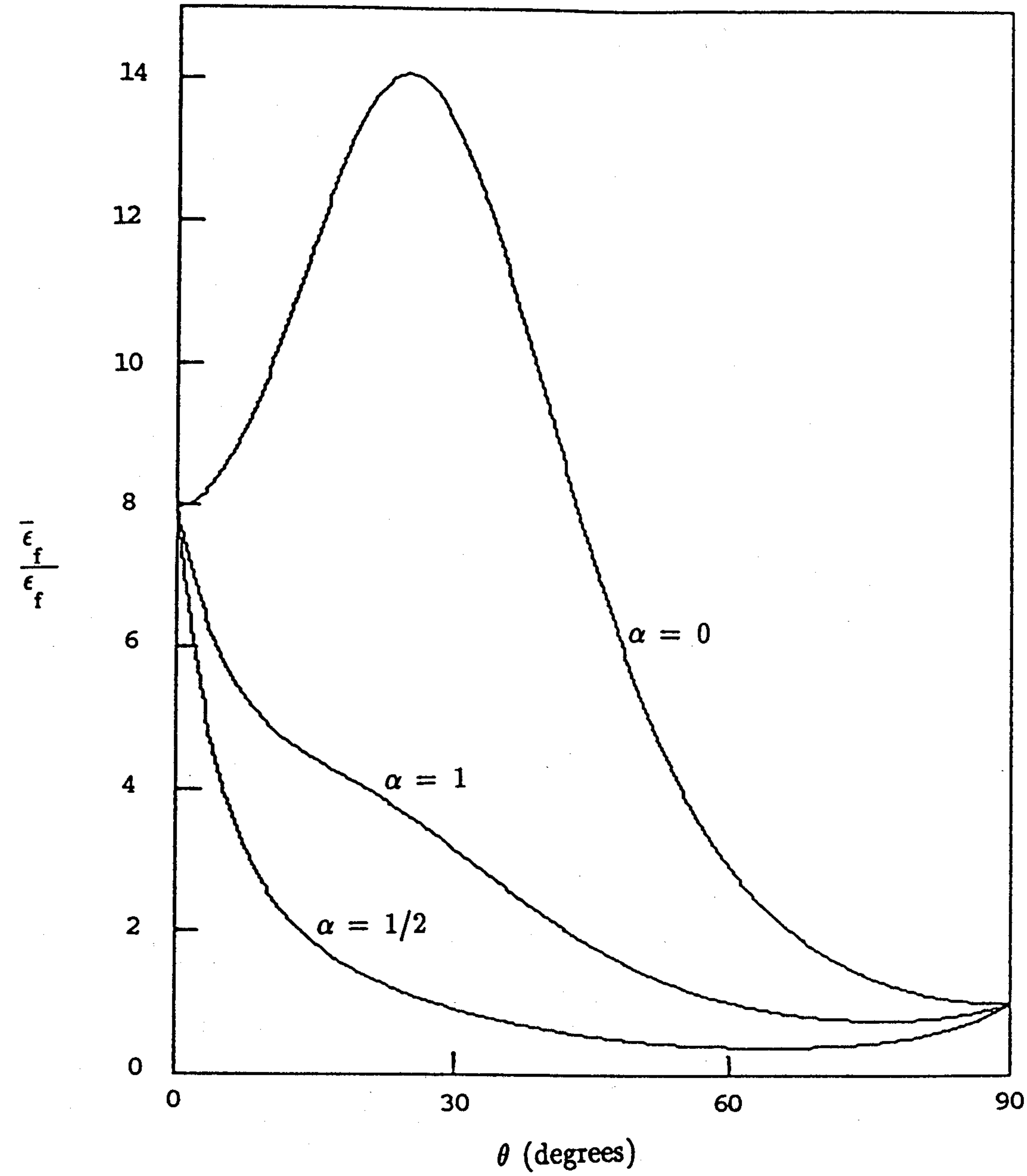

Figure 6. Dimensionless effective failure strain vs. θ. For $pR/\sigma_0 h = 1$, $n = 6$ and $\nu = 9$.

National Aeronautics and Space Administration	Report Documentation Page	
1. Report No. NASA CR-185286	2. Government Accession No.	3. Recipient's Catalog No.
4. Title and Subtitle: Creep and Creep Rupture of Strongly Reinforced Metallic Composites		5. Report Date: August 1990
		6. Performing Organization Code
7. Author(s): D.N. Robinson, W.K. Binienda, and M. Miti-Kavuma		8. Performing Organization Report No.: None
		10. Work Unit No.: 510-01-01
9. Performing Organization Name and Address: University of Akron, Akron, Ohio 44325		11. Contract or Grant No.: NAG3-379
		13. Type of Report and Period Covered: Contractor Report, Final
12. Sponsoring Agency Name and Address: National Aeronautics and Space Administration, Lewis Research Center, Cleveland, Ohio 44135-3191		14. Sponsoring Agency Code

15. Supplementary Notes

Project Manager, Steven M. Arnold, Structures Division, NASA Lewis Research Center.

16. Abstract

A creep and creep damage theory is presented for metallic composites with strong fibers. Application is to reinforced structures in which the fiber orientation may vary throughout but a distinct fiber direction can be identified locally (local transverse isotropy). The creep deformation model follows earlier work and is based on a flow potential function that depends on invariants reflecting stress and the material symmetry. As the focus is on the interaction of creep and damage, primary creep is ignored. The creep rupture model is an extension of continuum damage mechanics and includes an isochronous damage function that depends on invariants specifying the local maximum transverse tension and the maximum longitudinal shear stress. It is posited that at high temperature and low stress, appropriate to engineering practice, these stress components damage the fiber/matrix interface through diffusion controlled void growth, eventually causing creep rupture. Experiments are outlined for characterizing a composite through creep rupture tests under transverse tension and longitudinal shear. Applications is made to a thin-walled pressure vessel with reinforcing fibers at an arbitrary helical angle. The results illustrate the usefulness of the model as a means of achieving optimal designs of composite structures where creep and creep rupture are life limiting.

17. Key Words (Suggested by Author(s))	18. Distribution Statement
Creep; Creep rupture; Composites; Metallic; Viscoplasticity	Unclassified – Unlimited Subject Category 39

19. Security Classif. (of this report)	20. Security Classif. (of this page)	21. No. of pages	22. Price*
Unclassified	Unclassified	22	A03

NASA FORM 1626 OCT 86

*For sale by the National Technical Information Service, Springfield, Virginia 22161